Desalination and Water Treatment
www.deswater.com

doi: 10.5004/dwt.2020.25449

188 (2020) 140–150
June

RSM and ANN modeling of dissolved oxygen response using paper industry effluent in semi batch fermenter

J. Sumathi, M. Arulmozhi*, S. Sundaram

Department of Petrochemical Technology, Bharathidasan Institute of Technology (BIT) Campus, Anna University, Tiruchirappalli, India, email: arulmozhiphd@hotmail.com (M. Arulmozhi)

Received 3 May 2019; Accepted 10 January 2020

ABSTRACT

Effluent from paper industry was oxygenated till saturation using Lark Hygiene Fermenter at 25°C under real time environment. Time, speed, and feed concentration were selected as dominant input factors to determine the dissolved oxygen (DO) under response surface methodology (RSM) based Box–Behnken design to provide 17 experimental runs. The experimental results were optimized using RSM and artificial neural networks (ANN). From RSM analysis, a second-order quadratic representation for single objective optimization was successfully fitted which produced R^2 = 99.07 and R^2_{adj} = 97.87. Analysis of variance results shows that time and feed concentration were the most significant parameters than the speed, influencing the DO. Another single objective optimization tool ANN produced R^2 = 96.27 and R^2_{adj} = 94.06. Validation analysis provided the predicted values by RSM and ANN were close to the validation values, whereas RSM showed a better prediction than the ANN with the lowest deviation. Hence, the optimal condition predicted by RSM was taken to conduct the confirmatory experiment. The confirmatory experimental condition of time at 6 min, speed of 142 rpm with 90% concentration produced the minimal DO of 5.38 ppm. The error percentage of the predicted with confirmatory experimental and theoretical equations results were 1.11% and 0.035%, respectively, which validates the predicted model.

Keywords: Paper industry effluent; Semi batch fermenter; Box–Behnken design; ANN; DO

1. Introduction

Keeping in mind the environmental friendliness aspects of effluents released from any chemical industry, an attempt is made to optimize the dissolved oxygen (DO) in the effluents released from the paper industry. Contaminants can be detected at reduced concentrations and techniques to treat the same and to identify the degree of reduction of concentration to the required level are available [1]. When compared to the domestic and commercial waste waters, the industrial waste waters are highly polluted. The characteristics of the effluents differ from industry to industry as well as depend on the processes [2].

Contamination manifests via various medium, and mainly through water and air. The industrial waste water with various degrees of biochemical oxygen demand released from chemical processing industries, and other industrial units, is the major source of water pollution [3]. Saravanathamizhan et al. [4] employed artificial neural networks (ANN) and response surface methodology (RSM) modeling to study and develop the prediction model for electro-oxidation of Acid Red 88 dye house effluent using Ruthenium oxide-coated electrode in a CSTER; and confirmed the satisfactory matching of the ANN model, with the experimental observations. Ghosh et al. [5] investigated the ability to remove Cu^{2+} ions from aqueous solution using calcium oxide [$Ca(OH)_2$] treated orange peel and optimized the process

* Corresponding author.

parameters using RSM and ANN. Their optimization process showed a close interaction between the observational and modeled values of copper removal.

Huang et al. [6] research was conducted on urban river (Nanfei) in China. Authors were investigated, longitudinal profiles of DO and other related water constituents with high spatial goals observing at low stream. A DO model for the span was redone and aligned with the data obtained. Venkatesh Prabhu et al. [7] focused on the modeling and optimization of the decolorization procedure of real textile dye, and process parameters were optimized and compared using [8] a system model with two time-varying parameters used to relate the DO concentration in a bioreactor and model parameters were estimated using a regularized constant trace recursive least-squares method. An extended Kalman filter was used to remove the effect of noises from the DO concentration measurements and thus to improve control performance. Mondal et al. [9] investigated the removal of ranitidine hydrochloride from simulated pharmaceutical aqueous solution using steam-activated charcoal from mung bean husk by batch adsorption technique and showed that ANN has better prediction capability than RSM. Rokhina et al. [10] observed the pulp mill effluent treatment, using ruthenium on carbon, as the Novel Catalytic Adsorbent in the presence of hydrogen peroxide. They developed an optimization process and a mathematical process model with an orthogonal second-order design.

Arulmathi et al. [11] studied the electrochemical treatment optimization process and suggested that the COD and colour of distillery spent wash can be treated using T_i/P_t as an anode (batch mode) using RSM. Barrak et al. [12] observed that when reduced to industrial circumstances of the SITEX (Textile Industrial Company-Ksar Hellal, Tunisia), the treatment of Indigo dye (leuco form), reduced in the industrial circumstances through a batch electro coagulation with aluminum electrodes. For color removal [CR (%)] optimization they used RSM and BBD. Ahmad et al. [13] used RSM to study the coagulation–flocculation process optimization of palm oil mill effluent. Thirugnanasambandham et al. [14] experimented the application of RSM in the chemical coagulation process optimization in treating the waste water from the rice mill and to study meat industry waste water treatment by the enzymatic catalysis treatment method using lacasse.

Revollar et al. [15] proposed an IMC based PI control structure to improve the overall waste water treatment plant performance. The efficiency index considered as the proportion between the nitrogen expelled in the actuated sludge process and the energy required for taking out that measure of nitrogenated mixes and the efficiency index is used as the controlled variable in order to maintain the DO as close as possible to set point. Tony et al. [16] identified that one of the potentially useful oxidation process in the treatment of waste water effluents by RSM analysis, is the photo–Fenton's process. Tetteh et al. [17] focused the industrial mineral oil wastewater pre-treatment using RSM.

Guoweishu et al. [18] studied the effect of liquid, solid ratio, cellulose concentration, and reaction time on the extraction of jili polysaccharide from fruits of *Tribulus terrestris* L. Zahraee et al. [19] analyzed to integrate simulation modeling along with RSM and design of experiments in order to analyze and improve the productivity in a selected continuous paint manufacturing industry. Yang et al. [20] considered the real alkaline cleaning waste water for analysis and it was treated by a process consisting of neutralization, NaClO oxidation, and aluminum sulfate coagulation and a novel RSM coupled nonlinear programming approach was developed and used to optimize the oxidation–coagulation process under the constraints of relevant discharge standards.

Qiu et al. [21] used the application of Box–Behnken design (BBD) with RSM for modeling and optimizing ultrasonic oxidation of arsenite with H_2O_2. Saravani et al. [22] addressed the influence of various process parameters on the biosorptive foam separation performance of o–cresol onto *Bacillus cereus* and cetyl ammonium bromide using RSM. Wu et al. [23] addressed the application of the BBD to optimize the process parameters of foam cup molding. Suguna Nanthini et al. [24] developed an automated expert system using soft computing techniques such as fuzzy logic, neural network, evolutionary computation to analysis EEG signal classification. Mourabet et al. [25] used RSM for optimization of fluoride adsorption in an aqueous solution. Navamani Kartic et al. [26] addressed the importance of RSM and ASM modeling approach for pigment industry effluent. Nie et al. [28] projected their work on field studies of naidid distribution in a drinking water plant were conducted, and the effects of temperature and DO on naidid population dynamics were investigated using the life table method. Literatures show that very few studies reported quantitatively on the effect of dilution and the duration of aeration of DO [6]. This work investigated experimentally the effect of effluent to water ratio and its effect on DO. The significance of input function such as time, speed, and feed concentration toward the contribution of DO was analyzed using [18] BBD and ANN [5]. Based on the data analysis various models were analyzed and found that best fitted one is found to be a second-order quadratic model [11,17]. RSM and ANN were implemented to optimize the significant batch process.

2. Materials and methods

2.1. Experimental setup and procedure

Aeration and agitation are important variables to provide an effective oxygen transfer rate during aerobic processes [6]. Hence, the knowledge of the volumetric mass transfer coefficient (k_La) is required. Mass transfer and mixing are mostly influenced by stirrer speed, type and number of stirrers and gas flow rate used. Also, the knowledge of gas hold up (ϕ_G) in a bioreactor is essential in order to establish its aeration efficiency and to quantify the effects of operating variables on oxygen supply. In this work, DO level in the fluid is considered for analysis and is measured using DO probe, Lark Hygiene Fermenter, model: SS316L, 4–20 mA for inline measurement of oxygen in the reactor. The gas hold up is ϕ_G is obtained using Eq. (1), for Reynolds number = $\mathrm{Re}^{0.7}(\mathrm{Nd}_i/V_G)$ 0.3 < 30,000, is (Treybal [27]).

$$\phi_G = \left[0.24K\left(\frac{\mu_G}{\mu_L}\right)^{0.25}\left(\frac{V_G}{V_t}\right)^{\frac{1}{2}}\right]^{\frac{1}{(1-m)}} \quad (1)$$

V_G = superficial gas velocity (m/s); V_t = terminal settling velocity of a single bubble (m/s); μ_G = gas viscosity (kg/ms); μ_L = liquid viscosity (kg/ms).

And the k_La is determined using Eq. (2) [29]

$$k_La = 3.35\left[\frac{N}{N_{cd}}\right]^{1.464} V_G \quad (2)$$

where k_La is the volumetric gas–liquid mass transfer co-efficient, ($1s^{-1}$), N is the impeller speed, rps; N_{cd} is the minimum impeller speed for complete dispersion of the sparged gas, rps.

Further, the fractional DO is found out using Eq. (3) [30]

$$\ln(1-\mathrm{DO}) - \ln\left(\frac{C^*_{o2} - C^i_{o2}}{C^*_{o2}}\right) = -k_L \text{ at} \quad (3)$$

$$\mathrm{DO} = \left(\frac{C_{o2}}{C^*_{o2}}\right) \quad (4)$$

where DO is the fractional dissolved oxygen; C^*_{o2} is the concentration of oxygen at saturation in ppm; C^i_{o2} is the initial concentration in ppm. C_{o2} is the concentration of oxygen at any time t in ppm.

The DO concentration in ppm at time t can be calculated from Eq. (4). As air flows into the semi-batch reactor from the compressor, oxygen dissolves and obviously DO increases. Eq. (3) shows that a plot of ln(1–DO) vs. time is linear with negative slope equal to k_La. Based on theoretical analysis, real time experiment was carried out in semi batch fermenter.

The schematic diagram of the experimental set up for the process model used in this study shown in Fig. 1 and Table 1 shows semi-batch fermenter dimensions and the operating variables range of process setup which consist of a Lark hygiene fermenter, peristaltic pump, effluent storage, rotameter, DO probe, magnetic stirrer, control valve, and personal computer (PC). The 1.5 L fermenter has provisions for adjustment of air flow, temperature, and speed of the stirrer. Fresh effluent was diluted with water to obtain various feed concentrations ranging from 10% to 90% in steps of 40%.

One liter of the effluent of known feed concentration was charged into the fermenter from the storage tank using a peristaltic pump. The DO was monitored using an online Lark DO probe interfaced with a PC. At time $t = 0$, purified air was suddenly metered through a Gallenkamp rotameter at a rate of 1 Lpm. The DO was monitored and recorded for three inlet feed concentrations (10%, 50%, and 90%) and three speeds (135, 145, and 155 rpm) with respect to time till saturation (0, 15, and 30 min). The experimental data for the input of 90% feed concentration at speeds of 135, 145, and 155 rpm are shown in Fig. 2. Similar data were obtained for other effluent feed concentrations and speeds.

2.2. Experimental design employing BBD with RSM

For evaluating the relationship between input factors and responses (or) experimental outputs, [11,12] RSM is the

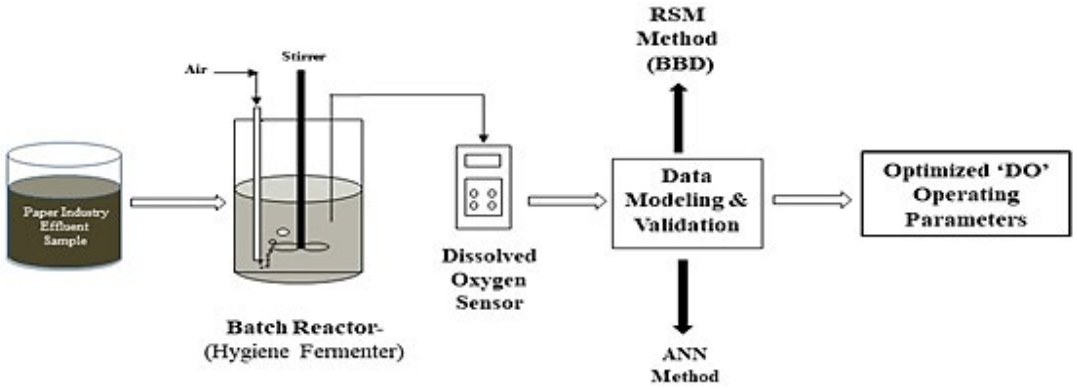

Fig. 1. Experimental setup for process model.

Table 1
Semi batch fermenter dimensions and operating variables ranges

Fermenter vessel	Total Volume: 3 L, $H \times D$: 250 × 150 mm
Mixing assembly	Contamination free with lip seals and Viton *V*-rings, two smooth bearings, two height adjustable ruston impeller with six blades each, three baffles
Aeration	Air sparger–*L*–type with Micro pores, Air outlet with 0.2 micro filter
Agitation	Stirrer motor PMDC, Speed range: 20–1000 rpm, Accuracy: 1 rpm
DO control	DO range: 0–100%, Accuracy: ±1% or 0.1 mg/L
Rotameter	Range: 0.5 to 5 L/min

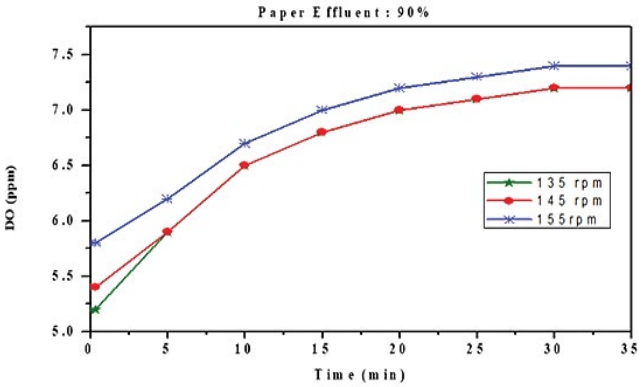

Fig. 2. Effect of variation of DO vs. Time for 90% paper effluent for 135, 145, and 155 rpm.

best suited empirical optimization technique. RSM method has adopted the combination of factorial design methods such as BBD and central composite designs [10,18]. Making use of BBD can precisely reduce the number of experimental sets without affecting the optimization accuracy when compared to the conventional factorial design method [21]. Table 2 illustrates the coded variables and uncoded variables with minimum and maximum ranges for three factors [23]. The following equations describe the relationship between the coded and uncoded variables.

$$a_1 = \frac{\left(A_1 - 15\right)}{15} \tag{5}$$

$$a_2 = \frac{\left(A_2 - 145\right)}{10} \tag{6}$$

$$a_3 = \frac{\left(A_3 - 50\right)}{40} \tag{7}$$

where A_1, A_2, and A_3 are the uncoded variables and a_1, a_2, and a_3 are the coded variables, respectively. Clearly, all three uncoded factors have their own units. To make the factors dimensionless, coded variables are introduced [17]. The effects of these three variables on the DO can be approximated using a quadratic model as shown in Eq. (6)

$$Y = b_0 + \sum_{i=1}^{n} b_i X_i + \sum_{i=1}^{n} b_{ii} X_{ii}^2 + \sum_{i<j} \sum_{j}^{n} b_{ij} X_i X_j \tag{8}$$

where Y = the predicted response (DO in ppm); b_0 = the offset term, b_i = the linear effect, b_{ii} = the square effect, b_{ij} = the interactive effect and X_i, X_j = the variables which are independent as well as coded [22,23].

2.3. ANN modeling

ANN is a machine learning technique with artificial neurons (processing units or elements) imitates the function of the human brain to perform a data classification process [5,7]. Feeding forward of neurons from one input layer to one output layer is called a perceptron. Perceptron is a linear classifier. Back propagation algorithm and perceptron are second generation neural network [9]. Back propagation technique is used as a model for the neural network in order to minimize the objective function [26]. Levenberg–Marquardt algorithm is used for training the network and the performance of the system is measured by using mean square error (MSE). The Levenberg–Marquardt algorithm works as follows: The algorithm also known as a damped least squares method. It works with a gradient vector and the jacobian matrix. It has been designed to work with loss function (sum of the squared errors).

Table 2
Three factors' minimum and maximum levels—in terms of coded and uncoded symbols.

Experimental variable	Variables		Levels		
	Coded	Uncoded	–1	0	1
Time (min)	a_1	A	0	15	30
Speed (rpm)	a_2	B	135	145	155
Concentration (%)	a_3	C	10	50	90

Consider the loss function of the form:

$$f = \sum e_i^2, i = 0,1,\ldots m \tag{9}$$

where m is the number of vectors in the data set.

Jacobean matrix of the loss function can be defined as:

$$J_{ij} f\left(w\right) = \frac{de_i}{dw_j}\left(i = 1,\ldots m; j = 1,\ldots n\right) \tag{10}$$

where m stands for the number of vectors and n stands for the number of parameters.

Therefore, we can compute the gradient vector of the loss function as:

$$\nabla f = 2J^t \times E \tag{11}$$

where E stands for error terms and J for Jacobean Matrix.

Finally, the approximation of the hessian matrix as;

$$\mathrm{Hf} \approx 2J^T \times J + \lambda I \tag{12}$$

Here, λ is the damping factor and I symbol stands for identity matrix. When λ is large, it becomes gradient descent with a small training rate.

Therefore, the parameters improvement process with the Levenberg–Marquardt as;

$$w_{i+1} = w_i - \left(J_i^T \times J_i + \lambda I\right)^{-1} \times \left(2J_i^T \times e_i\right) \quad i = 0,1,.. \tag{13}$$

A drawback of this algorithm is that it cannot be relevant to the root mean square error function. It requires a lot of memory when the data sets are big. Jacobean matrix will be huge for big data sets when we train the neural network.

The neural network tool in Matlab (R2016b) developed by the Math Works Inc., (Massachusetts, USA) was used in

this study. All possible combinations of parameters and values in Table 2 were taken and the number of experimental trials was 27. The network architecture consisted of one input layer with three inputs, one hidden layer with 10 neurons, and an output layer as shown in Fig. 3. The ratio of input data taken for training, validation, and testing was 70:15:15. Levenberg–Marquardt algorithm (trainlm) was used for training the network and the performance was measured using MSE. These parameters such as time, speed, and concentration are used for training the neural network. The performance of the model has been evaluated through MSE. The R^2 value predicted by ANN is 96.27 and R^2_{adj} is 94.06.

3. Results and discussion

The effects of time, speed, and feed concentration were estimated using BBD with RSM and ANN. Initially, to suggest a model to depict the relationships, considering the effects of interaction BBD with RSM and ANN were employed; so as to forecast and control the DO under various feed concentrations and different rotational speeds. Then, the influencing tendency of every factor is explored using RSM and ANN. Finally, the optimal conditions are determined for engineering use.

3.1. Optimization and determination of RSM

Experiments were carried out using the Box–Behnken experimental design. Table 3 shows the statistical summary of lack of fits for each model determined using Design Expert V8 software [14]. The experimental and predicted DO are tabulated in the experimental conditions as shown in Table 4. A second order quadratic model was suggested with the better R^2 and R^2_{adj} [21]. For a quadratic relationship, the R^2 and R^2_{adj} values were obtained as 99.07% and 97.87%, respectively; it is obviously evident that the quadratic relationship confirms the effects of interaction of input parameters and its percentage of contribution is tabulated in Table 5. In general, the significant parameters time, speed and concentration give a linear contribution, time, and concentration have a good interaction among themselves because of dependency on saturation along with the levels of time only. So, the time crucially involves in the saturation process to determine the DO levels. In other hand air when bubbled through the effluent creates the immense turbulence which provides effective mixing among them. Due to this external mixing with mechanical stirring, speed along with time or concentration does not have any impact to influence the DO levels. Hence, the level of saturation toward DO level existence clearly give a positive response toward the quadratic effect of time and concentration. As an evident from analysis of variance (ANOVA) Table 6, in our context linear, quadratic, and interactive effect among the chosen parameters contributed in their own way mechanism for the determination of DO levels. Hence, the quadratic model was identified.

3.1.1. Model fitting and analysis of variance

As per the analysis by the model, the data was fit the chosen quadratic [20]. The association between the DO and the three chosen parameters is shown in equation (14)

$$\text{Dissolved Oxygen} = +8.20 + 1.10 \times A - 0.25 \times B - 1.03 \times C - 0.075 \times AB - 0.18 \times AC + 0.23 \times BC - 0.44 \times A^2 - 0.088B^2 - 0.29 \times C^2 \quad (14)$$

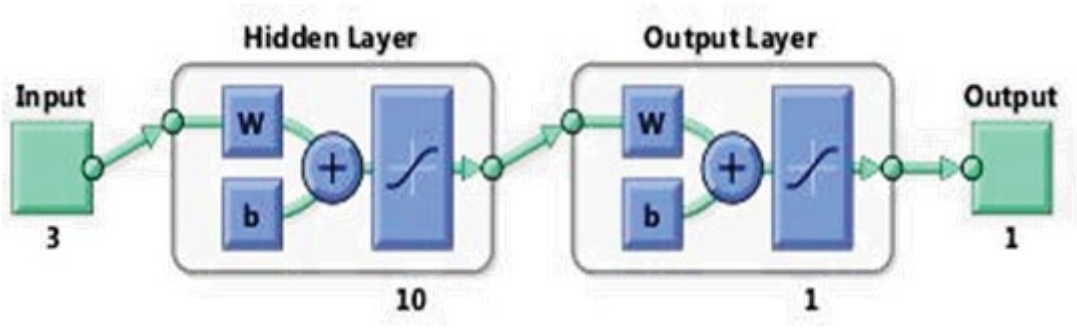

Fig. 3. Artificial neural network architecture.

Table 3
Statistical summary

Basis	Total of squares	Degree of freedom	Mean square	*F*-value	*p*-value prob > *F*	Suggestions
Linear vs. mean	20.13	3	6.71	51.66	<0.0001	
2F1 vs. linear	0.19	3	0.062	0.41	0.7493	
Quadratic vs. 2F1	1.39	3	0.46	27.53	0.0003	Suggested
Cubic vs. quadratic	0.12	3	0.039	6.366E+007	<0.0001	Aliased

Table 4
Experimental and predicted DO under different concentrations.

Run	Coded variables			Real variables			DO (ppm)	
	a_1 Time (min)	a_2 Speed (RPM)	a_3 Concentration (%)	*A* Time (min)	*B* Speed (RPM)	*C* Concentration (%)	Experimental	Predicted
1	0	–1	1	15	135	90	7.0	6.85
2	1	1	0	15	145	50	8.2	8.20
3	–1	0	–1	0	155	50	6.4	6.54
4	0	1	1	30	135	50	9.1	8.96
5	–1	1	0	0	145	10	7.4	7.34
6	–1	0	1	15	135	90	6.8	6.87
7	–1	–1	0	15	145	50	8.2	7.20
8	0	0	0	15	135	10	9.2	9.35
9	0	–1	–1	15	145	50	8.2	8.20
10	0	0	0	30	145	90	7.2	7.26
11	0	1	–1	30	155	50	8.5	8.59
12	1	0	1	0	135	50	6.7	6.61
13	0	0	0	15	155	10	9.0	8.92
14	0	0	0	15	145	50	8.2	8.20
15	1	0	–1	30	145	10	9.9	9.89
16	1	–1	0	15	145	50	8.2	8.20
17	0	0	0	0	145	90	5.4	5.41

Table 5
Analysis of variance results for acquired model

S.no.	Input parameters	Percentage of contribution (%)
1	Time	48.11
2	Speed	2.49
3	Concentration	41.78
4	Time and speed	0.11
5	Time and concentration	0.61
6	Speed and concentration	1.01
7	Time^2	4.01
8	Speed^2	0.16
9	Concentration^2	1.73

A, time in min; *B*, speed in rpm, and *C*, feed concentration in %.

The ratio, the explained variation to the total variation is defined as coefficient of determination (R^2); a measure of the degree of fit. When a model yields an R^2 of at least 0.9, it can be considered as a good model [19]. This means that, the process can be articulated in a well manner by the response model used in this investigation, at 95% confidence level, keeping R^2 = 99.07% and an R^2_{adj} = 97.87%. Additionally, it is palpable that this is a noteworthy model, from its value of F = 82.75 (F) model with the probability value as low as $p < 0.001$. The $p < 0.05$ is the clear indication that this model is statistically considerable.

A, *B*, *C*, *BC*, A^2, and C^2 are the noteworthy model from Table 6; the ANOVA results of the model obtained is shown. The coefficients for the quadratic terms for the time and feed concentration are indicated to be very significant, which infers that these factors have very big effects on the DO. Identification of dominant interaction effects study shows that the only interaction between time and feed concentration is more significant. This outcome also found that speed of stirring studies does not affect the time for saturation. Minimizing time of oxidation to achieve saturation in terms of DO helps in reducing power required for running the compressor. Stirring does not affect as seen because the bubbling of air itself creates turbulence and better mixing.

3.1.2. Model modification

After the significance of the parameters has been evaluated, the model can be improvised by eliminating the very less significant terms. The final model for describing the relationship between the time, speed, and feed concentration is shown in Eq. (15):

$$\text{Dissolved Oxygen} = + \ 8.16 + 1.10 \times A - 0.25 \times B - 1.03 \times C + 0.23 \times BC - 0.44 \times A^2 - 0.29 \times C^2 \quad (15)$$

Although, the R^2 value of 98.20 has decreased slightly, the R^2_{adj} = 97.12, which is a more important factor for determining the fit of a regression model, has changed from 97.87 to 97.12. Further P value of <0.001 denotes the more significant effect.

3.1.3. Model accuracy check

To obtain an ample model, an accuracy check is inevitable; by comparing the predicted and experimental DO the

Table 6
Analysis of variance results for acquired model

Basis	Total of squares	Degree of freedom	Mean square	*F*-model value	*P*-value prob > *F*	Characteristics
Model	21.70	9	2.41	143.66	<0.0001	Significant
A time	9.68	1	9.68	576.68	<0.0001	Most Significant
B Speed	0.10	1	0.10	6.03	0.0437	Significant
C Feed concentration	10.35	1	10.35	616.67	<0.0001	Most significant
AB	0.02	1	0.02	1.34	0.2849	Not significant
AC	0.12	1	0.12	7.30	0.0306	Significant
BC	0.04	1	0.04	2.38	0.1666	Not significant
A^2	1.16	1	1.16	69.14	<0.0001	Most significant
B^2	0.00	1	0.00	0.00	1.0000	Not Significant
C^2	0.17	1	0.17	10.03	0.0158	Significant
Residual	0.12	7	0.01			
Lack of fit	0.12	3	0.03			
Pure error	0.00	4	0.00			
Cor. total	21.82	16				

accuracy of the model was checked. Fig. 4 shows the linear association between the predicted and experimental DO. In addition, a normal plot of residuals between the normal probability (%) and the internally studentized residuals was also obtained.

In this way, the residuals can be checked to determine the degree that the model satisfies the assumptions of ANOVA, and the internally studentized residuals can be used to measure the standard deviations separating the experimental and predicted values. Fig. 5 Shows the association among the normal probability (%) and the residuals, which are studentized internally. No response transformation was required is inferred from the straight line and that there was no apparent problem with normality.

3.1.4. Response analysis

The relationships between the DO and these three factors are shown in Figs. 6–8. Every plot shows the effects of any two variables within their considered ranges, with the third variable fixed to the level of zero. The tendency of every factor in influencing the DO can be visualized better in the response surface. An elliptical contour plot points out a prominent interaction, among two variables. From the surface of response and contour plot, it is evident, that the interaction effects of time and feed concentration is more significant.

Figs. 6a and b indicate speed has little effect on DO saturation while Figs. 7a and b show that DO values change under feed concentration and time for a particular speed. Figs. 8a and b show once again that speed has little effect on DO variation with time and feed concentration. As it can be seen from these plots, speed is least significant factor as compared to feed concentration and time. Feed concentration and time plays a greater role in saturation of the effluent studied. This effect suggests that speed of stirring does not affect the time for saturation.

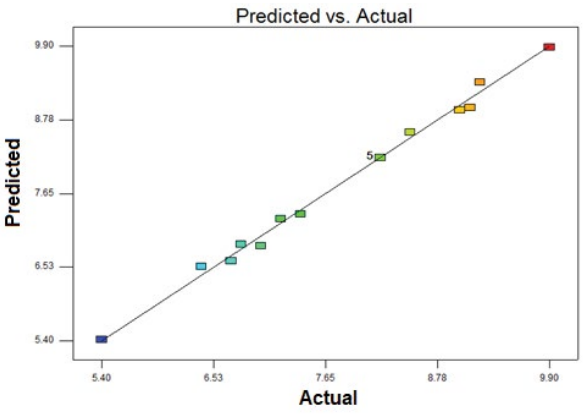

Fig. 4. Experimental and predicted data for paper effluent.

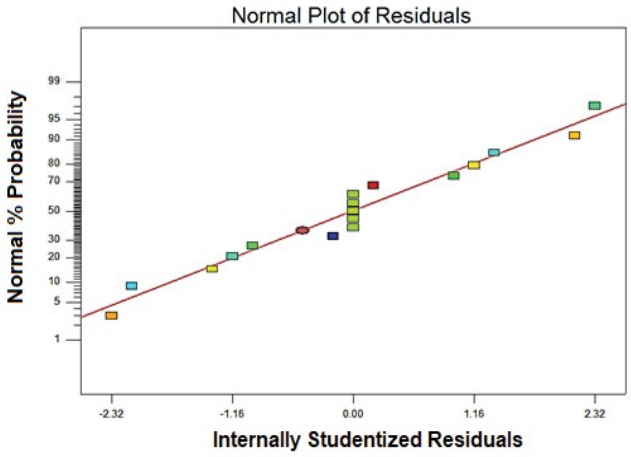

Fig. 5. Normal plot of residuals showing the relationship between normal probability (%) and internally studentized residuals.

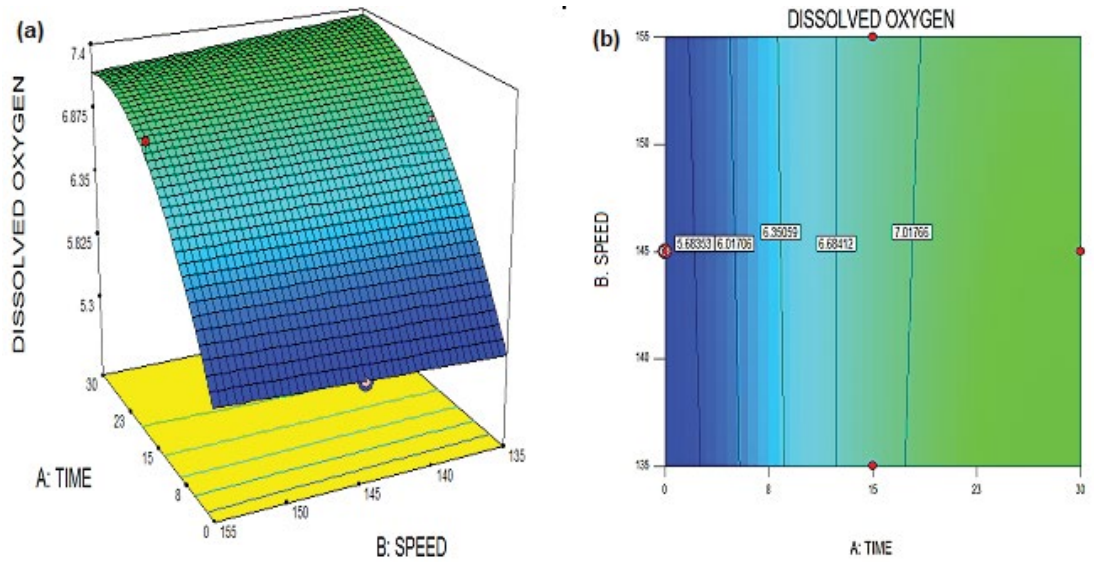

Fig. 6. (a and b) The surface and contour plot indicate that speed has little effect on DO saturation.

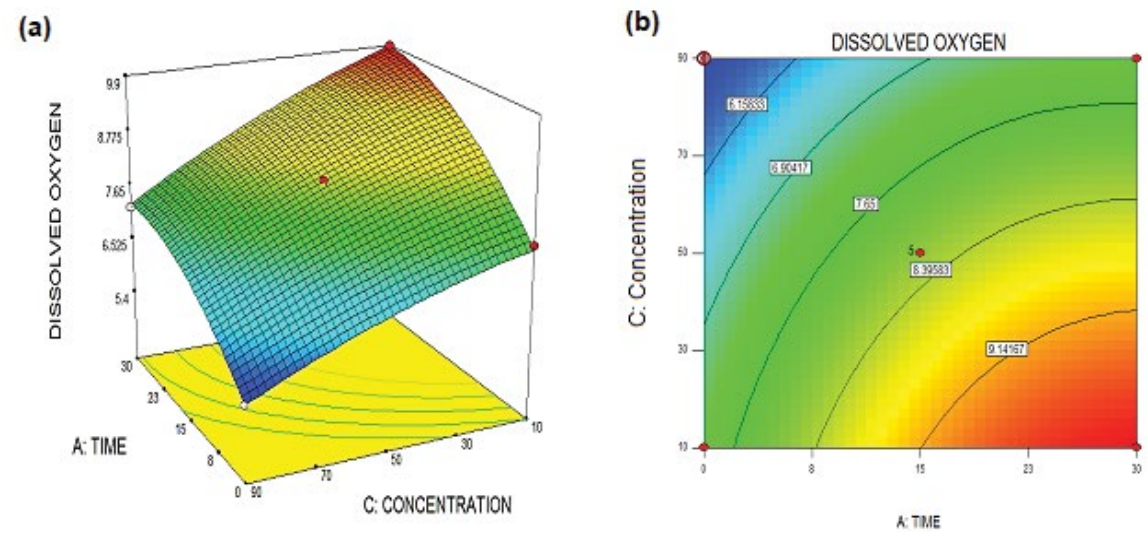

Fig. 7. (a and b) The surface and contour plot shows that DO vary under concentration and time for a particular speed.

3.1.5. Modeling by ANN

ANN was used to develop a mathematical model using all the responses obtained from the experimental results. Fig. 9 shows regression plots done by ANN for training validation, testing, and overall predicted model [26]. Predicted response for DO by ANN is shown in Table 7. It can be observed that the overall R^2 value for the model predicted by ANN was 96.27 and $R^2 = 94.06\%$; this model is suitable for modeling and optimizing paper industry effluent using DO as parameter. R^2 values of training and testing also suggest that the model was sufficiently trained and it holds good for prediction of new value. Both predictions by RSM and ANN model are close to the experimental results but the R^2 value of RSM prediction was higher than ANN prediction.

3.1.6. Condition optimization and confirmation tests

Based on the results of RSM and ANN, the predicted input factors were selected from RSM for the confirmatory experiment due to its closeness of fit (R^2 and R^2_{adj}), which is shown in Table 8. The Design Expert Software's optimization function was used to find out the minimized DO. The minimized DO of 5.32 was predicted at a time of 6.2 min, feed concentration of 90%, and speed of 142 rpm. The confirmatory trials were administered keeping condition optimum to validate the predicted result from the RSM optimization. The study infers that time and feed concentrations individually contributed toward the minimization of DO. The interaction effect of time is predominantly significant toward the different concentrations of effluent. The minimum DO shows the fine agreement among the experimental and predicted

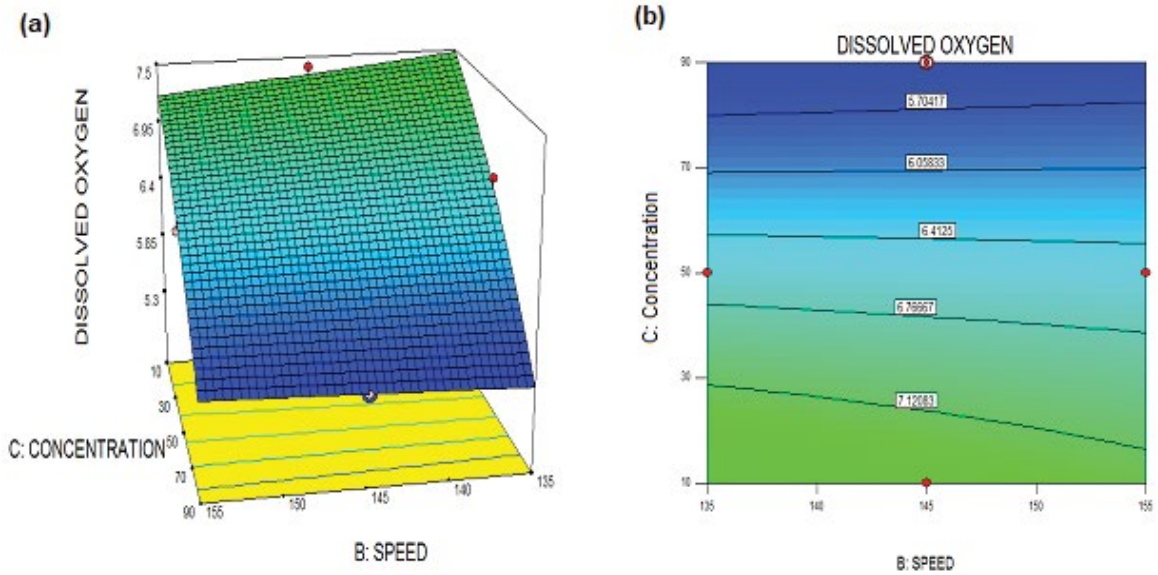

Fig. 8. (a and b) The surface and contour plot shows once again that speed has little effect on DO variation with time and concentration.

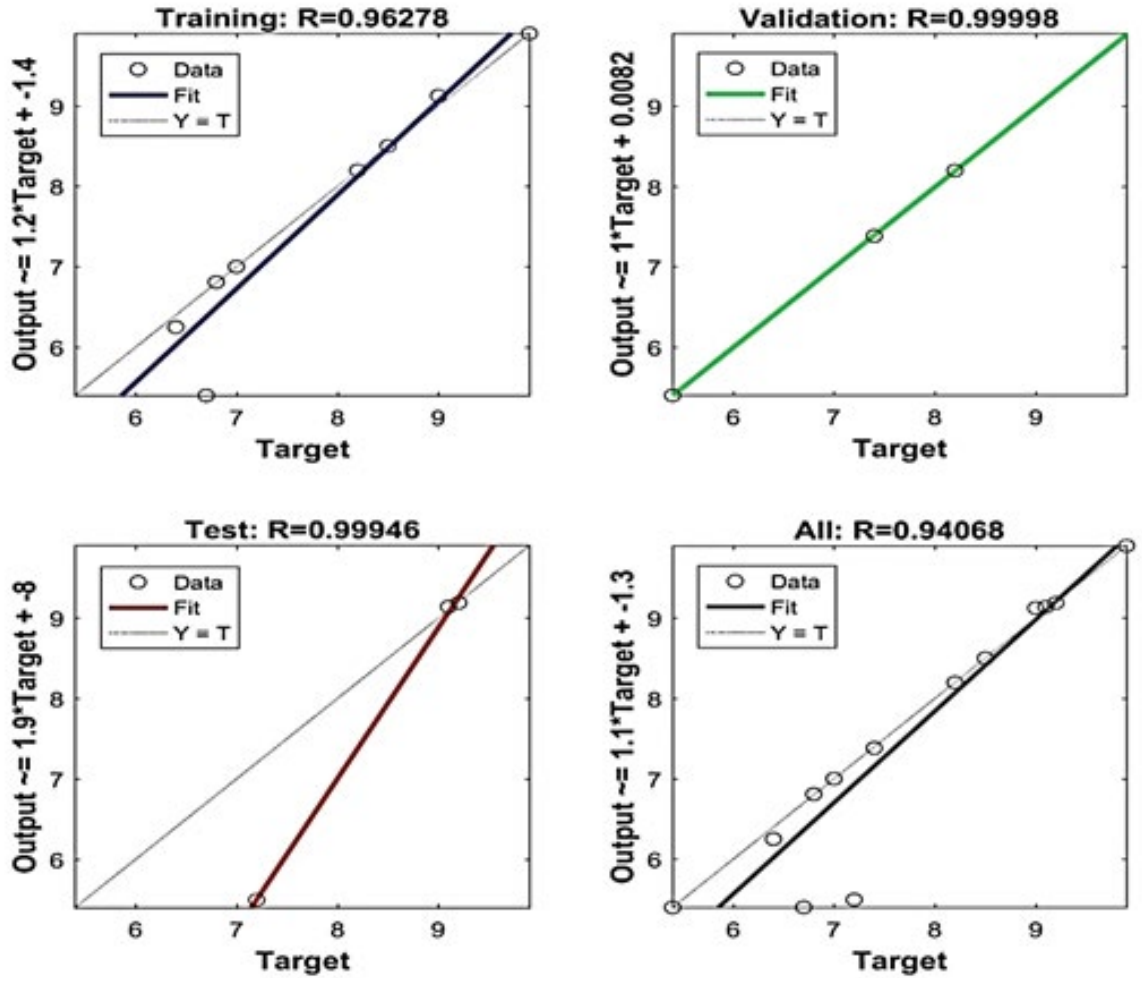

Fig. 9. Regression plots for ANN model.

Table 7
Predicted response for DO by ANN

A time (min)	*B* speed (RPM)	*C* concentration (%)	Experimental	Predicted
15	135	90	7.0	6.87
15	145	50	8.2	8.11
0	155	50	6.4	6.41
30	135	50	9.1	8.86
0	145	10	7.4	7.31
15	135	90	6.8	6.66
15	145	50	8.2	8.11
15	135	10	9.2	9.26
15	145	50	8.2	8.11
30	145	90	7.2	7.09
30	155	50	8.5	8.63
0	135	50	6.7	6.61
15	155	10	9.0	8.86
15	145	50	8.2	8.11
30	145	10	9.9	9.77
15	145	50	8.2	8.11
0	145	90	5.4	5.37

Table 8
Predicted and confirmatory experimental results for RSM

Result	Time (min)	Speed (rpm)	Concentration (%)	DO (ppm)	Theoretical DO (ppm) as per Eqs. (3) and (4) ([29,30])
Predicted result using RSM	6.2	142	90	5.32	5.625
Confirmatory experimental result	6.0	142	90	5.38	5.623
Error percentage (%)				1.11	0.035

Table 9
Comparison of predictive capacity of RSM and ANN

Parameters	RSM	ANN
RMSE	1.02	1.05
R^2	99.46	94.06
R^2_{adj}	98.77	94.26

results which authorizes the validity of the model with the error of 1.11%. From the predictive results on Table 9, it is obvious that RSM is a more powerful and effective tool for single objective optimization in a process, which is new.

4. Conclusion

This work investigates scientifically the effluent to water ratio effect on DO and the impact of stability of the process too, in a batch study. RSM and ANN models were implemented to optimize the batch process. Based on the various models, data were analyzed and the best suited is found to be the quadratic model. From RSM the model fitted the experimental data well, with a coefficient of determination, R^2 of 99.07% and R^2_{adj} of 97.87%. From ANOVA time and feed concentration were linearly influenced the DO, whereas speed and feed concentration provided an interactive effect on DO.

However, the predicted ANN model showed the R^2 of 96.27 and R^2_{adj} of 94.06, which ensures RSM prediction is performed better than ANN model. The optimal conditions predicted by RSM for DO, is at time 6.2 min, speed 142 rpm, and 90% feed concentration. The optimal response obtained from the RSM is very close to the confirmatory experimental value of 5.38. The error percentage obtained from the experimental and predicted value is 1.11% which validates the predicted and experimental data.

Acknowledgment

The authors express their gratitude for the financial support extended by the department of science and technology (DST–Government of India) Grant No. SR/FT/ETA-0017/2012 and Technical Education Quality Improvement Program (TEQIP II).

References

[1] F. Burton, G. Tchobanoglous, H. David Stensel, Waste Water Engineering Treatment and Reuse, 4th ed., McGraw-Hill, New York, 2002.

[2] S.K. Garg, Environment Engineering (Vol. II), Sewage Disposal and Air Pollution Engineering, Khanna Publishers, New Delhi, India, 2003.
[3] J. Sumathi, S. Sundaram, Effect of dilution and model analysis of distillery effluent using dissolved oxygen as parameter, Sens. Transducers J., 105 (2009) 113–118.
[4] R. Saravanathamizhan, K.H. Vardhan, D. Gnana Prakash, N. Bala Subramanian, RSM and ANN modeling for electro-oxidation of simulated wastewater using CSTER, Desalin. Water Treat., 55 (2015) 1445–1452.
[5] A. Ghosh, K. Sinha, P. Das Saha, Central composite design optimization and artificial neural network modeling of copper removal by chemically modified orange peel, Desalin. Water Treat., 51 (2013) 7791–7799.
[6] J. Huang, H. Yin, S.C. Chapra, Q. Zhou, Modelling dissolved oxygen depression in an urban river in China, Water, 9 (2017) 520.
[7] M. Venkatesh Prabhu, R. Karthikeyan, M. Shanmugaprakash, Modeling and optimization by response surface methodology and neural network–genetic algorithm for decolorization of real textile dye effluent using *Pleurotus ostreatus*: a comparison study, Desalin. Water Treat., 57 (2016) 13005–13019.
[8] S.C. Lee, Y.B. Hwang, H.N. Chang, Y.K. Chang, Adaptive control of dissolved oxygen concentration in a bioreactor, Biotechnol. Bioeng., 37 (1991) 597–607.
[9] S. Mondal, K. Aikat, G. Halder, Optimization of ranitidine hydrochloride removal from simulated pharmaceutical waste by activated charcoal from mung bean husk using response surface methodology and artificial neural network, Desalin. Water Treat., 57 (2016) 18366–18378.
[10] E.V. Rokhina, M. Sillanpaa, M.C.M. Bolte, J. Virkutyte, Optimization of pulp mill effluent treatment with catalytic adsorbent using orthogonal second-order (Box-Behnken) experimental design, J. Environ. Monit., 10 (2008) 1304–1312.
[11] P. Arulmathi, G. Elangovan, A. Farjana Begum, Optimization of electrochemical treatment process conditions for distillery effluent using response surface methodology, Sci. World J., 2015 (2015) 9.
[12] N. Barrak, R. Mannai, M. Zaidi, M. Kechida, A.N. Helal, Experimental design approach with response surface methodology for removal of indigo dye by electrocoagulation, J. Geosci. Environ. Prot., 4 (2016) 50–61.
[13] A.L. Ahmad, S. Ismail, S. Bhatia, Optimization of coagulation-flocculation process for palm oil mill effluent using response surface methodology, Environ. Sci. Technol., 39 (2005) 2828–2834.
[14] K. Thirugnanasambandham, V. Sivakumar, J. PrakashMaran, S. Kandasamy, Application of response surface methodology for optimization of chemical coagulation process to treat rice mill wastewater, Environ. Sci., 9 (2014) 237–247.
[15] S. Revollar, R. Vilanova, M. Francisco, P. Vega, PI Dissolved oxygen control in wastewater treatment plants for plantwide nitrogen removal efficiency, IFAC-PapersOnLine, 51 (2018) 450–455.
[16] M.A. Tony, Z. Bedri, Experimental design of photo-fenton reactions for the treatment of car wash wastewater effluents by response surface methodological analysis, Adv. Environ. Chem., 2014 (2014) 8.
[17] E.K. Tetteh, S. Rathilal, M.N. Chollom, Pre-treatment of industrial mineral oil wastewater using response surface methodology, Water Soc. IV, 216 (2017) 181–191.
[18] G. Shu, C. Dai, H. Chen, X. Wang, Application of Box–Behnken design in optimization for crude polysaccharides from fruits of *Tribulus terristris* L., J. Chem. Pharm. Res., 5 (2013) 342–350.
[19] S.M. Zahraee, J.M. Rohani, K.Y. Wong, Application of computer simulation experiment and response surface methodology for productivity improvement in a continuous production line: case study, J. King Saud Univ. Eng. Sci., 30 (2018) 207–217.
[20] Y. Yang, Z. Zhou, C. Lu, Y. Chen, H. Ge, L. Wang, C. Cheng, Treatment of chemical cleaning wastewater and cost optimization by response surface methodology coupled nonlinear programming, J. Environ. Manage., 198 (2017) 12–20.
[21] P. Qiu, M. Cui, K. Kang, B. Park, Y. Son, E. Khim, M. Jang, J. Khim, Application of Box–Behnken design with response surface methodology for modeling and optimizing ultrasonic oxidation of arsenite with H_2O_2. Ent. Eur. J. Chem., 12 (2014) 164–172.
[22] N. Saravani, M. Arulmozhi, Influence of various process parameters on the biosorptive foam separation performance of o–cresol onto *Bacillus cereus* and cetyl trimethyl ammonium bromide, J. Taiwan Inst. Chem. Eng., 67 (2016) 263–270.
[23] L. Wu, K.-l. Yick, S.-p. Ng, J. Yip, Application of the Box–Behnken design to the optimization of process parameters in foam cup molding, Expert Syst. Applic., 39 (2012) 8059–8065.
[24] B. Suguna Nanthini, EEG Signal Analysis for Automated Epileptic Seizure Detection using Soft Computing Techniques, Thesis, SASTRA University, Thanjavur, India, 2017.
[25] M. Mourabet, A. ElRhilassi, H. ElBoujaady, M. Bennani-Ziatni, A. Taitai, Use of response surface methodology for optimization of fluoride adsorption in an aqueous solution by Brushite, Arab. J. Chem., 10 (2017), S3292–S3302.
[26] D. Navamani Kartic, B.C. Aditya Narayana, M. Arivazhagan, Removal of high concentration of sulfate from pigment industry effluent by chemical precipitation using barium chloride: RSM and ANN modeling approach, J. Environ. Manage., 206 (2018) 69–76.
[27] R.E. Treybal, Mass Transfer Operations, 3rd ed., McGraw - Hill Book Company, Malaysia, 1981.
[28] X.-B. Nie, Y.-Q. Wu, Y.-N. Long, C.-B. Jiang, L. Kong, Impact of temperature and dissolved oxygen level on the population dynamics of naidids and their reproduction in biological activated carbon filters: a life table demographic study, Water Supply 19 (2019) 1363–1370.
[29] A.A. Yawalkar, A.B.M. Heeink, G.F. Versteeg and V.G. Pangarkar, Gas-liquid mass transfer coefficient in stirred tank reactors, Canad. J. Chem. Eng., 80 (2002) 840–848.
[30] L.A. Tribe, C.L. Briens, A. Margaritis, Determination of the volumetric mass transfer coefficient (k,a) using the dynamic "gas out-gas in" method: analysis of errors caused by dissolved oxygen probes, Biotechnol. Bioeng., 46 (1995) 369–392.